Block Shear and Net Section Capacities of Structural Tees in Tension: Test Results and Code Implications

HOWARD I. EPSTEIN and HANS STAMBERG

ABSTRACT

Structural tees in tension, bolted to connections only through the flanges, are subject to shear lag. Previous research has shown that shear lag, a reflection of connection length, overall length and the eccentricity to the centroid, strongly influence the efficiency of such connections. This paper reports the results of 50 tests of structural tees. Varying the eccentricity and the connection length produced failures that transitioned from net section to block shear. The tests show that as connection lengths decrease or eccentricities increase, or both, the efficiency of the connections decreases. For net section failures, the decrease is more pronounced than predicted by current AISC specifications provisions that use the $(1 - \bar{x}/l)$ factor (with a lower limit) to account for eccentricity and connection length. Although not accounted for by current AISC specifications, eccentricity is also shown to influence block shear capacity. The primary purposes of this paper are to present test results and possible alternative approaches to dealing with the areas of tension connection efficiency and shear lag.

INTRODUCTION AND BACKGROUND

The work that is reported in this paper has roots in investigations of block shear failures in angles (Thacker, 1987; Epstein and Thacker, 1991; Adidam, 1990; Epstein, 1992). These led to a limited series of tests to determine whether tees that are connected through their flanges would produce block shear failure results similar to pairs of angles. Unlike angles, when block shear failures occurred for the tees tested, only one shear plane was present (Twilley, 1996; Epstein, 1996). The failure mode was termed *alternate* path block shear failure (ABS). This study of tees led to the more extensive testing program reported herein. In this investigation, eccentricities and connection lengths were systematically varied.

Howard I. Epstein is professor, department of civil and environmental engineering, University of Connecticut, Storrs, CT.

Hans Stamberg is engineer, Virginia Vermiculite, Louisa, VA.

Before any further tests were designed, finite element studies of structural tee sections were done to try to predict the mode of failure (McGinnis, 1998; Epstein and McGinnis, 2000). The finite element models accurately predicted relative loads and failure modes for the previously tested series. The finite element models also predicted the previously undocumented alternate block shear failure path. An interesting result found in this study was that for deep tees there is a compression zone in the web at the section containing the lead bolt holes. Furthermore, it was determined that the moment caused by the eccentricity is not simply equal to the load multiplied by the eccentricity, but is partially reduced by the opposing moment caused by the rotationally restrained connection. An analytic equation for the moments present in an eccentrically loaded tee in tension was subsequently determined (D'Aiuto, 1999; Epstein and D'Aiuto, 2002).

A previous study (Epstein, 1992) suggested that either increasing the eccentricity (hence the resulting moment) or decreasing the connection length diminished the block shear capacity of angles. These factors, however, are yet to be incorporated in any AISC Specification equations. The study of tees initially was designed to investigate block shear. Although test results for tees were showing that eccentricity and connection length were also influencing capacity, similar to their effects for angles, it soon became apparent that the ability to predict moments could be directly applied to net section failure paths. The resulting equation for the moment (Epstein and D'Aiuto, 2002) then was used for net section tension failures in tees. It was shown that the capacity of tee connections may be based on current interaction equations for combined moment and axial force, rather than the tension equations that incorporate shear lag factors. Shear lag factors, in effect, are a measure of the efficiency of the connection (i.e., the predicted capacity compared to capacity based on net area times ultimate strength). Using the combined moment and axial force, an efficiency relationship was derived and the results obtained by using these factors were compared with those using the shear lag factors.

The present paper reports the results of destructive tests performed on 50 structural tee sections at the University of Connecticut. These specimens had varying eccentricities and connection lengths and the failures transitioned from net section to block shear (alternate). The test results are compared with current AISC Specification equations and possible implications are discussed. Only the *Load and Resistance Factor Design Specification for Structural Steel Buildings* will be referred to in this paper (AISC, 1999). However, any descriptions or conclusions reached regarding LRFD specifications are equally applicable to the ASD Specification treatment (AISC, 1989).

The LRFD design strength for yielding of the gross section is given by

$$\phi P_n = \phi_{ty} F_y A_g \tag{1}$$

where
- P_n = nominal axial strength
- ϕ_{ty} = resistance factor for yielding = 0.9
- F_y = specified minimum yield strength
- A_g = gross area

When there is a reduction in cross-sectional area, such as for bolt holes, net section failure strength is given by

$$\phi P_n = \phi_{tf} F_u A_e \tag{2}$$

where
- ϕ_{tf} = resistance factor for fracture = 0.75
- F_u = specified minimum ultimate strength
- A_e = effective net area

The net area, A_n, is reduced to the effective net area using the shear lag reduction factor, U, through the equation

$$A_e = UA_n \tag{3}$$

where
- U = $1 - \bar{x}/l \le 0.9$
- $\bar{x}$ = connection eccentricity
- l = connection length

The shear lag factor may also be given by specific values, according to the commentary to the LRFD specification. These values (0.75 or 0.85) are herein given by the symbol U^* and are used whenever the computed U produces a lower value.

Birkemoe and Gilmor (1978) observed a new failure mode for the connection of a coped beam. This failure, termed *block shear*, involved tearing of the base metal along the perimeter of the bolt holes. They suggested an equation for strength that combines tensile strength on one plane with shear strength on the perpendicular plane. While the treatment of block shear has undergone modest modifications over the years, specification equations for strength remain similar to those originally posed. The current LRFD specification (AISC, 1999) uses for nominal strength, R_n,

$$\phi R_n = \phi[0.6 F_y A_{gv} + F_u A_{nt}] \le \phi[0.6 F_u A_{nv} + F_u A_{nt}], \quad \text{when } F_u A_{nt} \ge 0.6 F_u A_{nv} \tag{4a}$$

and

$$\phi R_n = \phi[0.6 F_u A_{nv} + F_y A_{gt}] \le \phi[0.6 F_u A_{nv} + F_u A_{nt}], \quad \text{when } 0.6 F_u A_{nv} > F_u A_{nt} \tag{4b}$$

where
- ϕ = 0.75
- A_{gv} = gross area subjected to shear
- A_{gt} = gross area subjected to tension
- A_{nv} = net area subjected to shear
- A_{nt} = net area subjected to tension

Prior to the 1999 specification, the block shear strength was based on the fracture of the net tension or shear area together with yield of the remaining gross area (AISC, 1994). Now, the block shear strength also is limited to that obtained from fracture of both net areas.

EXPERIMENTAL PROGRAM

For this study it was considered desirable to test tees that were likely to fail in alternate block shear and then vary the depths and connection lengths to transition to net section failures. All connections were designed to fail by either net section or block shear, in accordance with current LRFD specifications. The 50 tee sections were fabricated from W10×12 (34 tees), W12×16 (12 tees) and W12×19 (4 tees) wide flange sections. While standard tees are cut from wide flange sections along the centroidal axis of the web, many of the tee sections for this study were intentionally not fabricated as standard tees. The wide flange sections were cut parallel to the centroidal axis, in one-in. increments, resulting in tee sections with depths larger and smaller than standard. Varying the web depth allows the effect of eccentricity to be studied while all other connection and section geometries are held constant. If block shear is the failure mode, reducing the depth eventually will lead to a net section failure.

Geometry

A typical specimen is shown in Figure 1 (the bolt holes at the far end are not shown). The connections had four, six, or eight bolts, in drilled holes, in two gage lines, one in each flange. The length of all specimens (L) was 53 in. The pitch (p) for the specimens was 3 in., except for nine sections that had a 4.5-in. pitch. The resulting connection lengths (l) were 3-in. (these connections had four bolts), 4.5-in. (these connections also had four bolts), 6-in. (these connections had six bolts) or 9-in. (these connections had 8 bolts). The gage (g) was 2.25 in. for all of the specimens. Although A325 bolts probably would have been sufficient for the connections, ¾-in. A490 bolts were used to help insure against bolt failure. All sections had a 1.5-in. edge distance (e).

Specimen Groupings

The tests were grouped and assigned specimen numbers according to the connection length and the wide flange section from which they were fabricated. The only variable in these "E-series" is the depth (hence the eccentricity). For each connection length, specimens are listed according to descending web depths. The specimen groupings and number designations are shown in Table 1. Specimens numbered 1 through 34 are standard and non-standard WT5×6 sections. Series E1 (numbered 1 through 10) have 3 in. connections, E2 (numbered 11 through 19) have 4.5 in. connections, E3 (numbered 20 through 27) have 6 in. connections, and E4 (numbered 28 through 34) have 9 in. connections. Specimens numbered 35 through 44 are standard and non-standard WT6×8 sections with 3 in. connections (Series E5). Specimens numbered 45 and 46 are standard WT6×8 sections with 6 in. and 9 in. connections, respectively. Specimens numbered 47 through 50 are standard and non-standard WT6×9.5 sections with 3 in. connections (Series E6).

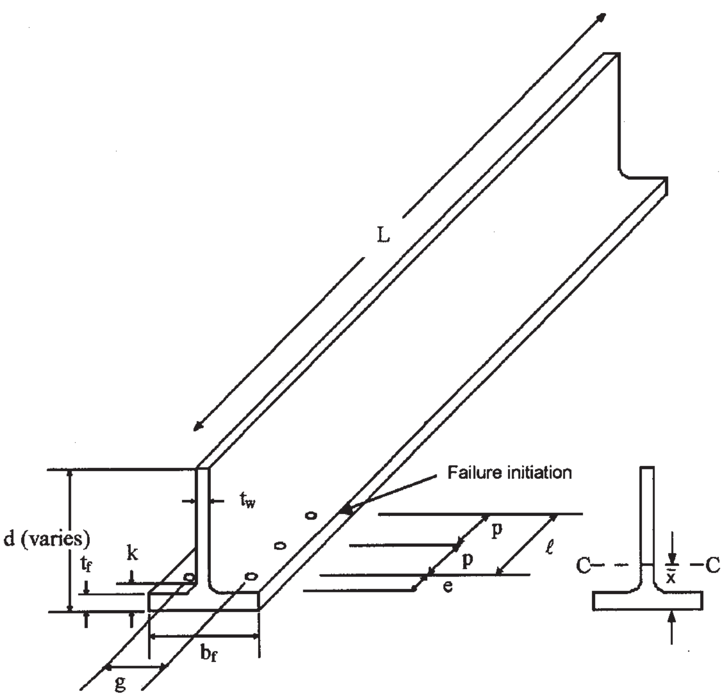

Fig. 1. Typical specimen geometry.

The specimens also were grouped according to web depth. In these "C-series" designations, the only variable is the connection length. These designations also are indicated in Table 1. For instance, the C1 series (consisting of specimens numbered 2, 12, 20 and 28) are non-standard WT5×6 with depths 3 in. greater than a standard WT5×6 (hence the +3 designation) with varying connection lengths (3 in., 4.5 in., 6 in. and 9 in., respectively).

Shear Lag Reduction Factors

Also shown in Table 1 are the eccentricities, $\bar{x}$. The eccentricities are 1.36 in., 1.74 in. and 1.65 in. for the WT5×6, 6×8 and 6×9.5 standard sections, respectively. For the non-standard sections, the eccentricities shown in Table 1 are derived from

$$\bar{x} = [A_s x_s + N t_w (d_s + N/2)]/[A_s + N t_w] \tag{5}$$

where

A_s = area for the standard section
d_s = depth for the standard section
x_s = eccentricity for the standard section
N = additional depth of the section (e.g., for specimen #1, N = +4 and for #7, N = -1)
t_w = web thickness

Table 1 also shows the computed value of $U = 1 - \bar{x}/l$. Note that some of the sections have such a large eccentricity, compared to the connection length, that the computed U values are very low. In fact, the computed U for specimen #1 is actually negative. As stated previously, since the code allows the designer to use U^* = 0.75 for the four-bolt connections and 0.85 for the six- and eight-bolt connections, these U^* values were used whenever they were higher than the computed U.

Material Properties

Berlin Steel (Berlin, Connecticut) donated three 40-ft W10×12, three 10-ft W12×16 and one 10-ft W12×19 wide flange sections from which all 50 specimens were fabricated. To obtain material properties, standard 19-inch long tensile coupons were taken from the webs of the W sections. The strengths of the three W12×16 sections were almost identical and were probably cut from one larger section. The average yield and ultimate strength of the W12×16 sections is 57.8 ksi and 69.2 ksi, respectively. One W10×12 section had a yield strength of 57.6 ksi and an ultimate strength of 78.0 ksi. The other W10×12 section had a

Table 1. Specification Capacities and Test Results (kips)

#	Series	Section	l (in.)	$\bar{x}$ (in.)	U $1-\bar{x}/l$	Specification Capacities				Test Results		PF
						NS	ABS	Design Load	Failure mode	Failure Load	Failure Mode	
1	E1	WT5x6+4	3.0	3.03	-0.01	94.3	56.4	56.4	ABS	87.3	ABS	1.16
2	E1/C1	WT5x6+3	3.0	2.60	0.135	86.0	56.4	56.4	ABS	85.1	ABS	1.13
3	E1/C2	WT5x6+2	3.0	2.17	0.277	77.7	56.4	56.4	ABS	81.7	ABS	1.09
4	E1/C3	WT5x6+1	3.0	1.76	0.415	69.4	56.4	56.4	ABS	86.8	ABS	1.15
5	E1/C4	WT5x6	3.0	1.36	0.547	61.1	56.4	56.4	ABS	76.8	NS	1.02
6	E1/C4	WT5x6	3.0	1.36	0.547	61.1	56.4	56.4	ABS	83.0	NS	1.10
7	E1/C5	WT5x6-1	3.0	0.99	0.670	52.9	56.4	52.9	NS	80.4	NS	1.14
8	E1/C6	WT5x6-2	3.0	0.66	0.781	46.4	56.4	46.4	NS	79.2	NS	1.28
9	E1/C7	WT5x6-3	3.0	0.37	0.875	42.4	56.4	42.4	NS	74.2	NS	1.31
10	E1	WT5x6-4	3.0	0.17	0.942	33.6	56.4	33.6	NS	62.6	NS	1.40
11	E2	WT5x6+4	4.5	3.03	0.326	94.3	73.7	73.7	ABS	97.0	ABS	0.99
12	E2/C1	WT5x6+3	4.5	2.60	0.423	86.0	73.7	73.7	ABS	103.8	NS	1.06
13	E2/C2	WT5x6+2	4.5	2.17	0.518	77.7	73.7	73.7	ABS	89.2	NS	0.91
14	E2/C3	WT5x6+1	4.5	1.76	0.610	69.4	73.7	69.4	NS	96.9	NS	1.05
15	E2/C4	WT5x6	4.5	1.36	0.698	61.1	73.7	61.1	NS	96.4	NS	1.18
16	E2/C5	WT5x6-1	4.5	0.99	0.780	55.0	73.7	55.0	NS	99.8	NS	1.36
17	E2/C6	WT5x6-2	4.5	0.66	0.854	50.7	73.7	50.7	NS	86.1	NS	1.27
18	E2/C7	WT5x6-3	4.5	0.37	0.917	43.6	73.7	43.6	NS	76.8	NS	1.32
19	E2	WT5x6-4	4.5	0.17	0.961	33.6	73.7	33.6	NS	66.0	NS	1.47
20	E3/C1	WT5x6+3	6.0	2.60	0.567	97.5	83.6	83.6	ABS	115.4	NS	1.04
21	E3/C2	WT5x6+2	6.0	2.17	0.639	88.1	83.6	83.6	ABS	114.0	NS	1.02
22	E3/C3	WT5x6+1	6.0	1.76	0.708	78.7	83.6	78.7	NS	105.6	NS	1.01
23	E3/C4	WT5x6	6.0	1.36	0.773	69.3	83.6	69.3	NS	102.4	NS	1.11
24	E3/C4	WT5x6	6.0	1.36	0.773	69.3	83.6	69.3	NS	104.9	NS	1.14
25	E3/C5	WT5x6-1	6.0	0.99	0.835	59.9	83.6	59.9	NS	96.8	NS	1.21
26	E3/C6	WT5x6-2	6.0	0.66	0.891	53.5	83.6	53.5	NS	84.8	NS	1.19
27	E3/C7	WT5x6-3	6.0	0.37	0.938	43.6	83.6	43.6	NS	76.4	NS	1.31
28	E4/C1	WT5x6+3	9.0	2.60	0.712	97.5	103.5	97.5	NS	132.3	NS	1.02
29	E4/C2	WT5x6+2	9.0	2.17	0.759	88.1	103.5	88.1	NS	126.6	NS	1.08
30	E4/C3	WT5x6+1	9.0	1.76	0.805	78.7	103.5	78.7	NS	118.6	NS	1.13
31	E4/C4	WT5x6	9.0	1.36	0.849	69.3	103.5	69.3	NS	110.9	NS	1.20
32	E4/C5	WT5x6-1	9.0	0.99	0.890	62.7	103.5	62.7	NS	101.2	NS	1.21
33	E4/C6	WT5x6-2	9.0	0.66	0.927	53.5	103.5	53.5	NS	86.8	NS	1.22
34	E4/C7	WT5x6-3	9.0	0.37	0.958	43.6	103.5	43.6	NS	75.8	NS	1.30
35	E5/C8	WT6x8	3.0	1.74	0.420	73.8	64.3	64.3	ABS	89.5	ABS	1.04
36	E5/C8	WT6x8	3.0	1.74	0.420	73.8	64.3	64.3	ABS	93.3	ABS	1.09
37	E5/C8	WT6x8	3.0	1.74	0.420	73.8	64.3	64.3	ABS	93.6	ABS	1.09
38	E5	WT6x8-1	3.0	1.35	0.549	65.2	64.3	64.3	ABS	91.9	ABS	1.07
39	E5	WT6x8-1	3.0	1.35	0.549	65.2	64.3	64.3	ABS	91.7	ABS	1.07
40	E5	WT6x8-1	3.0	1.35	0.549	65.2	64.3	64.3	ABS	91.1	ABS	1.06
41	E5	WT6x8-2	3.0	0.99	0.669	56.7	64.3	56.7	NS	87.6	ABS	1.16
42	E5	WT6x8-2	3.0	0.99	0.669	56.7	64.3	56.7	NS	87.6	NS	1.16
43	E5	WT6x8-3	3.0	0.67	0.777	49.8	64.3	49.8	NS	87.4	NS	1.32
44	E5	WT6x8-3	3.0	0.67	0.777	49.8	64.3	49.8	NS	86.5	NS	1.30
45	C8	WT6x8	6.0	1.74	0.710	83.7	89.9	83.7	NS	110.1	ABS	0.99
46	C8	WT6x8	9.0	1.74	0.807	83.7	110.5	83.7	NS	123.8	NS	1.11
47	E6	WT6x9.5	3.0	1.65	0.450	81.8	70.4	70.4	ABS	135.1	ABS	1.44
48	E6	WT6x9.5-1	3.0	1.29	0.571	72.3	70.4	70.4	ABS	126.8	NS	1.35
49	E6	WT6x9.5-2	3.0	0.96	0.682	63.6	70.4	63.6	NS	123.6	NS	1.46
50	E6	WT6x9.5-3	3.0	0.66	0.780	57.0	70.4	57.0	NS	118.8	NS	1.56

yield strength of 59.0 ksi and an ultimate strength of 77.0 ksi. Since the properties of these two sections were almost identical, the average values of the yield and ultimate strengths, 58.3 ksi and 77.5 ksi, respectively, were used to simplify the comparison of results. The W12×19 had yield and ultimate strengths of 49.8 ksi and 66.2 ksi, respectively.

Classification of Failures

Failures for all 50 specimens initiated at the free edges of the flanges in the section containing the leading bolt holes (see Figure 1). When these sections ruptured, the load decreased and as the displacement increased, the failure propagated to encompass the entire flange. Pictures of the failed specimens in the E2 series (#11 through #19) are shown in Figure 2. For the smallest web depth (specimen #19), the failure was net section. As the web depth increased, the failure in the web is seen to veer at an ever-increasing angle. As long as the end of the specimen is not involved, the failure was classified as net section (NS). Once the end of the specimen is involved (specimen #11), the failure mode was classified as alternate block shear (ABS). The failure loads and failure modes are shown in Table 1. Note that the side view of failed specimens #11 and #12 clearly shows web distortions out of plane. For all specimens that had large web depth to width ratios, local buckling clearly occurred before failure initiation.

Specification Design Capacities

Either net section or block shear failure, on the alternate path, governed the computed design capacities for all 50 specimens. Therefore, the capacities corresponding to yielding of the gross cross section, bolt failure, and the two-shear-plane block shear failure are not shown in Table 1. Contained in Table 1 are the net section capacities, using the maximum of U or U^*, and the alternate block shear capacities, using the latest AISC Specification treatment of Equation 4(a) or 4(b).

A sample calculation for the net section capacity of specimen #6 (a standard WT5×6 with a 3 in. connection) was previously presented (Epstein and D'Aiuto, 2002). To compute the block shear capacity for this specimen, note that the gross tension area is the gross area of the WT less $(d-k)t_w$, the area of the web not in the block shear failure path. Then, A_{gt} = 1.77 − (4.935 − 0.625)(0.19) = 0.951 in.^{2} The net tension area is then the gross tension area less two holes in the flange, which for two ¾ in. bolt holes on a 0.21-in. thick flange is 2(0.875)(0.21) = 0.368 in.^{2} Thus, A_{nt} = 0.951 − 0.368 = 0.583 in.^{2} For the alternate block shear path, the net

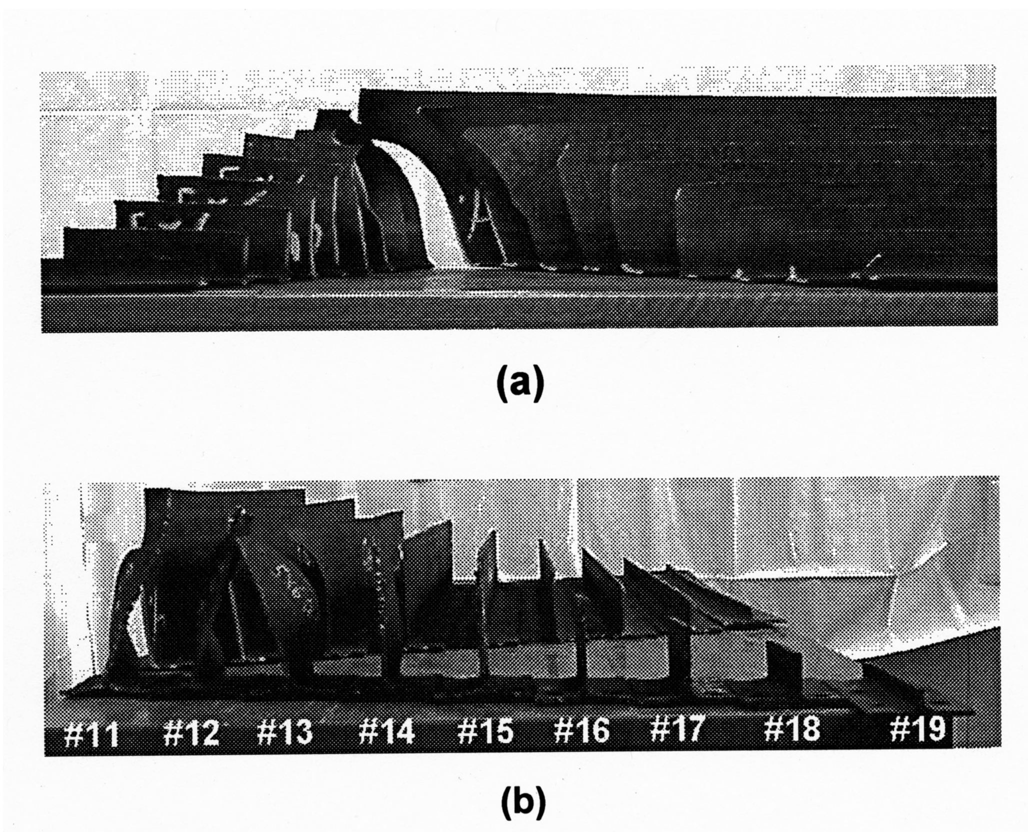

Fig. 2. Failed specimens in series E2 (specimens #11 through #19).

shear area equals the gross shear area of $(l + e)t_w$. It follows that $A_{nv} = A_{gv} = (3+1.5)(0.19) = 0.855$ in.^{2} Equation 4a then gives the block shear capacity, since $A_{nt} > 0.6A_{nv}$. The nominal capacity is then $R_n = [0.6(58.3)0.855 + 77.5\ (0.583)] = 75.1$ kips, resulting in $\phi R_n = 0.75(75.1) = 56.3$ kips, and since $A_{nv} = A_{gv}$ and $F_u > F_y$, the second capacity in Equation 4a does not govern. The net section capacity was found to be 61.1 kips (Epstein and D'Aiuto, 2002), which is, therefore, the design capacity for section #6.

Table 1 presents all the design capacities along with their associated failure modes of either net section (NS) or alternate block shear (ABS). Note that the block shear capacities do not depend on the depth of the web and, hence, the eccentricity of the connection. For instance, specimens #1 through #10 all have the same value for ABS.

Note to Future Researchers

The thesis on which this paper is based (Stamberg, 2000) was presented before the 1999 specification was available. The introduction in 1999 of the check for fracture on both net areas (shear and tension) reduces some of the capacities shown in the thesis. Since $A_{nv} = A_{gv}$ for ABS, whenever Equation 4a governed there was no change. All 3 in. connections in this study (e.g., the example just presented) are governed by Equation 4a and, therefore, are unchanged. However, when Equation 4b governed (all 4.5 in., 6 in. and 9 in. connections), there was a reduction in ABS capacity. Since NS still governed most of these longer connections, there were only five specimens in which the capacity was reduced (#11, #12, #13, #20 and #21). In two of these (#13 and #21) the predicted failure mode changed from NS to ABS, with a corresponding reduction in capacity (5.2 percent and 5.1 percent, respectively). The reduction in capacity for sections #11, #12 and #20 were 9.9 percent, 9.9 percent and 8.8 percent, respectively. All five of these specimens (and one other) had predicted capacities greater than the test values, and now three remain.

Test Results

The failure loads and failure modes for all 50 specimens are presented in Table 1. As can be seen, the specification failure modes were in substantial agreement with test results. In fact, only nine of the 50 specimens failed in a mode different than predicted (seven predicted as ABS failed in NS and two the reverse). The last column of Table 1 shows Professional Factors (*PF*), defined as the ratio of experimental failure load to predicted failure load, P_{test}/P_n (Galambos, 1981). For instance, for specimen #6, $PF = 83.0/75.2 = 1.104$.

Comparison of Tests with Specifications

There are many ways in which the data presented above can be analyzed. For example, results can be grouped according to predicted or actual failure modes. Results also can be presented by varying only the eccentricities (E series) or varying only the connection length (C series). Results can be presented using Professional Factors (*PF* values), actual test to specification ratios (these differ from *PF* values by the ϕ factors) or according to connection efficiencies (not very meaningful when block shear is the failure mode). This paper presents several ways of looking at the results.

Results for Varying Eccentricities (E series)

Figure 3(a) shows a plot of nominal (without the ϕ factors) specification values for the E1 series as the web depth of the tee varies from four in. less than standard (−4) to four in. greater (+4). The E1 series consists of specimens #1 through #10. The design capacities for each individual specimen previously were shown in Table 1.

Figure 3(a) shows how each of the specification capacity equations varies with web depth. There are four curves shown in this figure. The straight line labeled *Alternate Block Shear* is merely the capacity shown in the ABS column of Table 1, which for these specimens is 56.4 kips divided by the ϕ factor of 0.75, producing a nominal ABS capacity of 75.2 kips. The three curves labeled "Net Section …" are merely net section design capacities, F_uA_nU. The three curves differ by the value of U used: the maximum value of 0.9, the commentary value of 0.85 (U*) for this four-bolt connection, or the varying $\left(1-\bar{x}/l\right)$ factor in the specification. Note that for a constant U (either 0.85 or 0.9) as the web depth increases so does the net section capacity and the resulting plots are straight lines with positive slopes. For the plot of varying U, however, the net section is increasing, but $\left(1-\bar{x}/l\right)$ is decreasing. This produces a curve that, for this series, increases to a maximum and then decreases. For the E1 series, the resulting capacity is governed by net section for web depths less than standard and alternate block shear for the standard and greater than standard web depths. For the net section, $U = 0.9$ governs for the −4 specimen (#10), $U = 1-\bar{x}/l$ for the −3 and −2 specimens (#9 and #8) and $U = 0.85$ for the −1 specimen (#7). The resulting nominal capacity, as a function of the web depth variation, is shown as four solid line segments in Figure 3(a).

This nominal capacity plot is reproduced in Figure 3(b) together with the actual test capacities. As can be seen, the failure mode was accurately predicted except for the standard depth (specimens #5 and #6). The test results divided by the nominal capacities produce the Professional Factors (*PF*) shown in Table 1. Thus, values below 1.0 are not conservative. Plots for other E series are similar to those just presented in Figure 3 (Stamberg, 2000) except that in series E4, ABS never governs and series E5 and E6 do not include positive web variations.

Figure 4 shows *PF* versus web depth variation for all six E series. Note that wherever there were duplicate tests (e.g., #5 and #6, #23 and #24, etc.), an average value was taken. The general trend of the *PF* values is a decrease with increasing web depths (eccentricities).

Results for Varying Connection Lengths (C series)

Figure 5 shows *PF* values versus connection length for all eight C series. These values, on the average, diminish slightly from the 9 in. to the 3 in. connection. Again, it can be seen that there are lower values for the more eccentric connections (C1, C2 and C3 series have depths greater than standard) and higher values for the less eccentric connections (C6, C7 and C8 series have depths less than standard). Plots of the nominal capacities versus connection length (not shown herein) are complicated by the jump that sometimes occurs in ABS values when there is a change in which equation governs, Equation 4a or 4b.

PF vs $\left(1-\bar{x}/l\right)$

The effects of connection length and eccentricity both are contained in $U = 1 - \bar{x}/l$, the shear lag factor in the current AISC Specifications. Figure 6 shows the plot of *PF* versus *U* for all 50 specimens (some of the results overlay). The crosses represent NS failures (36 specimens) and the circles ABS failures (14 specimens). The blackened points are tests where the mode of failure was not the same as the governing specification equation. Seven of the 36 NS failures had design capacities governed by ABS and two of the 14 ABS failures had NS predicted capacities.

LRFD is predicated upon a resistance, ϕ, factor that assures that only a minute subset of tests will result in failure loads less than the nominal capacity times this ϕ factor. If there were no specification treatment for a particular failure mode, the ϕ factor would be determined to ensure the adequacy of the provision. For connections, ϕ is set at 0.75. Thus, as an ideal, one would want *PF* to average approximately $1.0/\phi = 1.0/0.75 = 1.33$ and with little scatter.

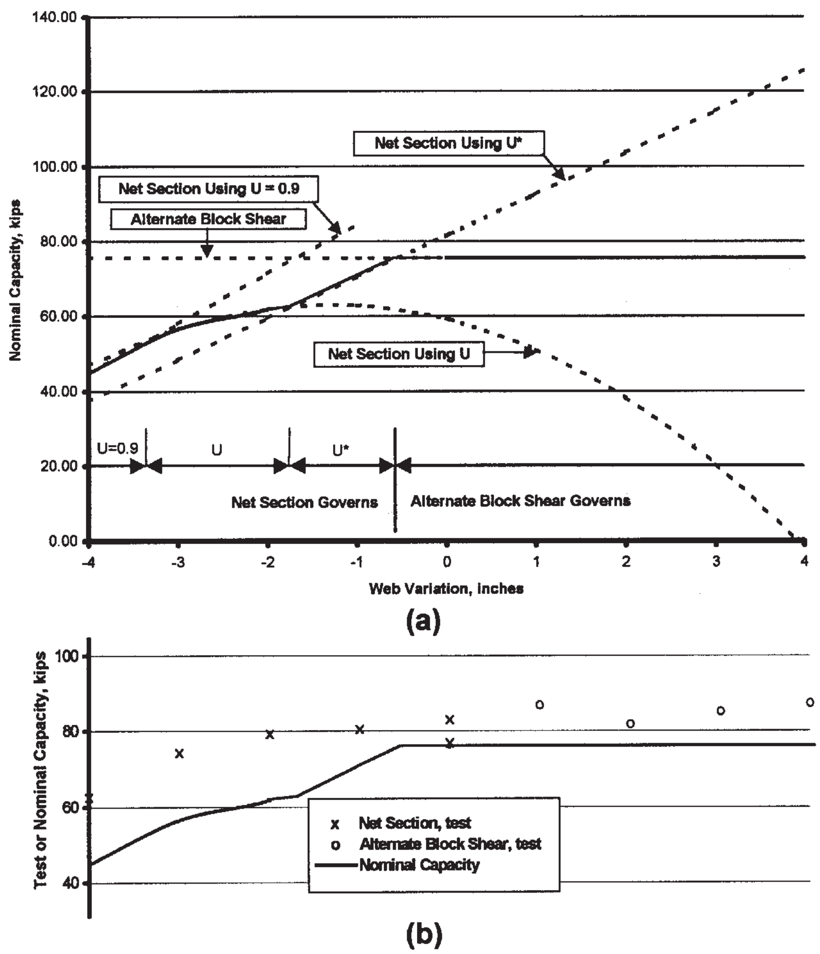

Fig. 3. Test results and nominal capacities versus web depths.

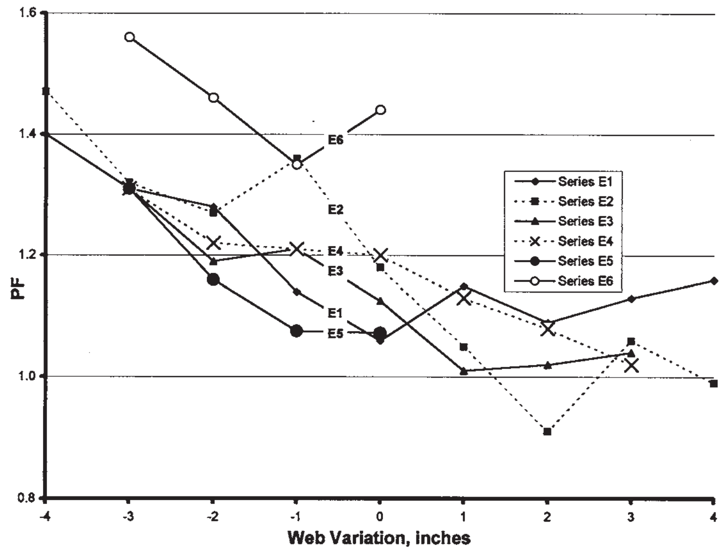

Fig. 4. E series professional factors versus web depths.

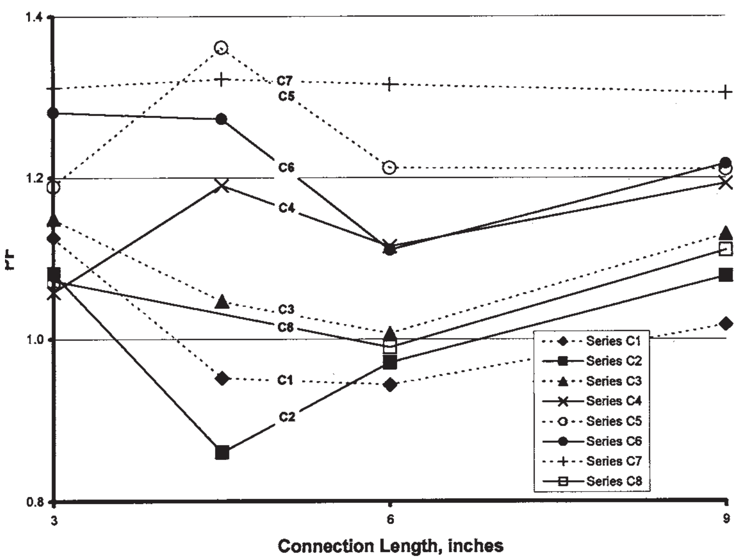

Fig. 5. C series professional factors versus connection lengths.

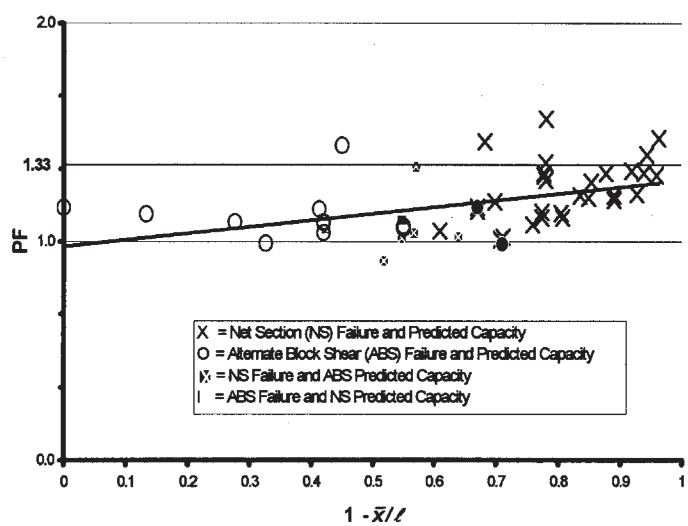

Fig. 6. Professional factors versus $1 - \bar{x}/l$ for all 50 specimens.

For the current test results, there should not be the trend of diminishing *PF* values for connections with smaller *U* values (shorter connections and/or connections with more eccentricity). When this diminishing trend was previously seen for block shear failure in angles (Epstein, 1992) it was suggested that the inclusion of the *U* factor in the tension terms of Equations 4a and 4b produced results that were more satisfactory. Now, it also appears that even for NS failures in structural tees, where *U* is the measure of connection efficiency, the AISC Specification treatment may not be sufficient for those connections with lower *U* values. There are a few tests with PF falling below 1.0 and several others that are close. If more tests were conducted for geometries that produce small *U* values, it is probable that the results would cause concern.

POSSIBLE SPECIFICATION TREATMENTS

Only structural tees are presented herein and any suggested modification should include provisions for all structural shapes. However, the trends noted for tees are exactly what has been seen for angles, namely that large connection eccentricity or small connection lengths, or both, seem to diminish test/capacity ratios. Any proposed modifications should consider test results of other shapes and should either be applicable to low values of *U* or those values somehow should be specifically treated or excluded.

One previous study for tees (Epstein and D'Aiuto, 2002) showed that the moment in tees for an applied load (P) at an eccentricity $(\bar{x})$ could be presented as a function of many factors including connection length (l), overall length (L), the elastic and shear modulus of the material (E and G), depth (d) and web thickness (t_w). This moment is given by

$$M = \left(1 - \frac{\left(\frac{l^2}{2EI} \left(L - \frac{3}{2} l \right) \right)}{\left(\left(\frac{l^2}{6EI} (3L - 4l) \right) + \left(\frac{l}{\lambda G t_w d} \right) \right)} \right) Px \tag{6a}$$

where

$$\lambda = \frac{(\ell - d)}{\ell}, \text{ for } l > 2d, \text{ and} \tag{6b}$$

$$\lambda = \frac{\ell}{4d}, \text{ for } l \le 2d \tag{6c}$$

or

$$M = \beta P \bar{x} \tag{7}$$

where β is the term in the large brackets in Equation 6a. These analytic moments account for shear deformation in the vicinity of the connection and simply reduce to $P\bar{x}(\beta = 1)$ when connections are completely free to rotate. Recently completed research at The University of Connecticut (Barrett, 2002) has shown that the equations for moments in tees appear to be appropriate for angles as well. When these analytic equations for moments are substituted into present LRFD moment-axial force interaction equations, the result is

$$\frac{\phi P_u}{\phi_t P_n'} \le \left(\frac{1}{1 + \left(\frac{8}{9} \right) \left(\frac{\phi_t}{\phi_b} \right) \left(\frac{F_u}{F_y} \right) \left(\frac{\bar{x} A_n}{Z} \right) \beta} \right) = U \equiv U_L \tag{8}$$

where

$P_n' = F_u / A_n$
$\phi_t/\phi_b = 0.75/0.9$
Z = section modulus

A similar expression ($U = U_A$) was derived for the ASD interaction equation (Epstein and D'Aiuto, 2002).

Equation 8 represents a new reduction factor that is based on the moments caused by the eccentricity of the load and the bending and tensile capacities of the section. U_L measures connection efficiency and serves a similar function to the shear lag factors U or U^* currently used in the LRFD specification. The shear lag factor was introduced to account for cross sections that had insufficient shear stiffness to develop the ultimate stress over the entire cross sectional area. Shear rarely is present without bending. Logically, shear lag is also related to bending. Shear and bending are both represented in $(1 - \bar{x}/l)$ because $\bar{x}$ is a measure of bending and both $\bar{x}$ and l are related to shear stiffness. The shear area (depth and width of the web) is also a factor in the amount of shear lag present. Equation 8 incorporates the actual shear stiffness.

It is certainly not being suggested here that the analytic equation for moments or the resulting reduction factor U_L be part of any future AISC Specification, as they are far too complex. However, these do present an analytic tool to be used in conjunction with current and previous experimental programs to possibly produce amended specification treatments for net section and block shear capacities of connections.

When U_L was applied in place of U or U^* to the NS failures shown in this present study, the results were much improved (Stamberg, 2000). The Professional Factors had much less variation with connection length and eccentricity, and on average were closer to the ideal value of 1.33. When U_L was applied to the tension terms of the block shear equations, the results for ABS were also improved. The approach of incorporating the shear lag factor, U, into block shear first was presented in the study of angles (Epstein, 1992). A plot similar to Figure 6 but using U_L for NS and the tension areas in ABS is seen elsewhere (Stamberg, 2000).

The primary purposes of this paper are to present test results and possible alternative approaches to dealing with the areas of tension connection efficiency and shear lag. For another approach, consider the plot shown in Figure 7. This figure compares, for the 50 specimens tested, the values of $U = 1 - \bar{x}/l < 0.9$, $U^* = 0.75$ or 0.85, and U_L from Equation 8. Connections with low calculated values of U probably would be designed for the allowable U^* values, hence the designation of "probable shear lag values" in this figure. The calculations for the U_L values use the material properties previously given and also use $E = 29{,}000$ ksi and $G = 11{,}200$ ksi. Also, all needed dimensions were previously given and geometric properties for other than the standard sections are easily obtained (e.g., Equation 5 gives $\bar{x}$) and all may be found elsewhere (Stamberg, 2000).

If one accepts the premise that the use of U_L improves the specification treatment but is too complex for routine design use, then a plot similar to that in Figure 7 may be very helpful in finding alternative equations for U in terms of $(1 - \bar{x}/l)$. For instance, one possible set of equations that are still fairly simple could be

$$LB \le 1 - \alpha\, \bar{x}/l \le UB \tag{9}$$

where LB and UB are lower and upper bounds, respectively, and α changes the slope of the graph in Figure 6. In fact, Equation 9 was used in lieu of U or U^* to determine the capacity of the 50 specimens tested. This factor also was applied to all NS failures and to the tension terms in the ABS failures. The upper bound was set at 0.9 and LB and α were varied to see what values produced a minimum in the least square variation of PF values from 1.33. Two sets gave similar low values: (A) $\alpha = 1.3$ with $LB \cong 0.7$, and (B) $\alpha = 1.0$ with $LB \cong 0.65$. Set (B) certainly is only a modest change to the present AISC Specification and it also follows the U_L points in Figure 6 fairly well. Therefore, based on this very limited set of tests, a possible treatment for shear lag could be to simply eliminate the U^* values and in addition to the current upper bound place a lower bound on U, thus giving

$$0.65 \le U = 1 - \bar{x}/l \le 0.9 \tag{10}$$

This treatment led to much more acceptable trend lines for plots, similar to Figure 6, of PF versus $(1 - \bar{x}/l)$ for NS or ABS failures or both plotted together (Stamberg, 2000). Remember that the ABS predicted capacities decrease when any U factor, less than one, is applied to the tension terms in Equation 4a or 4b.

CONCLUSIONS AND RECOMMENDATIONS

This paper reported the results of tension tests of 50 structural tees. The tees were bolted to connections only through the flanges. Varying the eccentricity and the connection length produced failures that transitioned from net section to block shear (alternate). The tests demonstrated that as connection lengths decreased or eccentricities increased or both, the efficiency of the connections decreased.

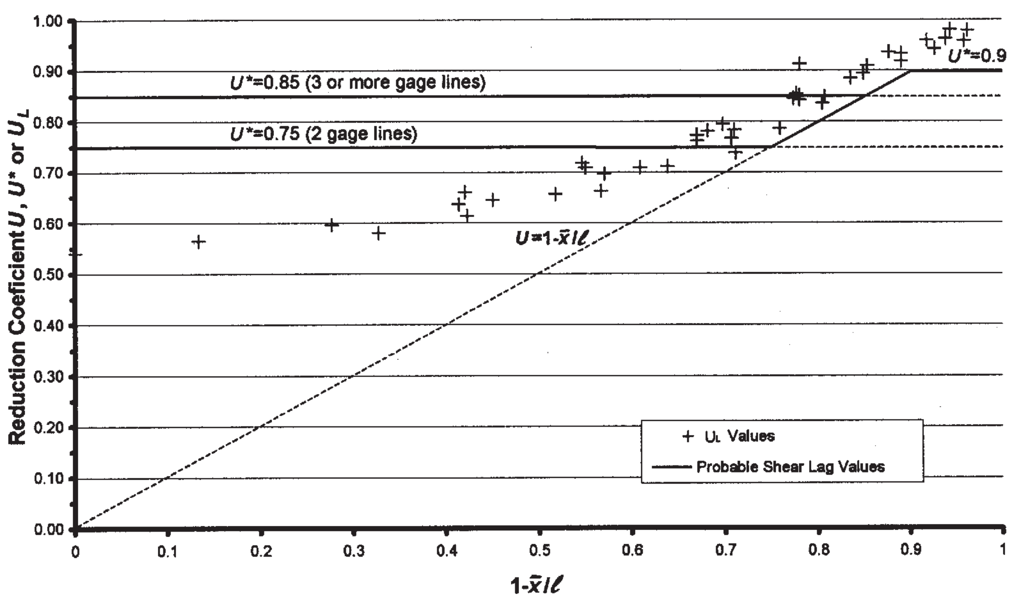

Fig. 7. U_L compared with specification values.

For net section failures, this decrease is more pronounced than what is predicted by current AISC Specifications that use the $(1-\bar{x}/l)$ factor (with upper and lower limits) to account for eccentricity and connection length. Also, the professional factors decreased to levels substantially below desired levels for decreasing values of $(1-\bar{x}/l)$. For alternate block shear failures, professional factors were consistently below ideal values. Sections with large eccentricity had local buckling before the failure load was reached and, therefore, for tensile loading, a limit on depth-to-width ratio for the web appears to be needed.

Eccentricity also was shown to influence block shear capacity, a factor that is not accounted for by current AISC Specifications. As concluded in a previous study, when block shear failures result from loads that are eccentric to the plane of failure, there appears to be a need to account for this eccentricity.

Using analytically derived moments, a possible new treatment for specifying capacity was shown. For the current set of tests, the use of $0.65 \le U = 1-\bar{x}/l \le 0.9$ produced very acceptable results when used for the efficiency of net section failures and as a factor on the tension area in block shear failures.

It is recommended that if $1-\bar{x}/l$ is not used but, instead, tabulated U values are employed, lower values than the current 0.75 and 0.85 should be adopted. For very short connections or those with large load eccentricities, $1-\bar{x}/l$ can become very small, and even may be negative. Obviously the use of $1-\bar{x}/l$ makes no sense for such connections. It is recommended that the Specification lead the designer to employ interaction equations for such cases. Finally, block shear equations must recognize that the eccentricity of the load, either in plane or out of plane, decreases capacity. It is recommended that a U factor be applied to the tension area of the block shear equations.

ACKNOWLEDGMENTS

The authors are indebted to the National Science Foundation (Project #CMS-9610474), the American Institute of Steel Construction and The University of Connecticut Research Foundation for their sponsorship of the research that led to this paper. Special thanks are owed to the Berlin Steel Construction Company of Berlin, CT, for donating the WT specimens used in the testing program, B & F Machine of New Britain, CT, for donating the material and machining the pallets needed to grip the specimens, and to the School of Engineering machine shop staff. Finally, thanks to Rebecca Zwerling for invaluable editorial input.

REFERENCES

Adidam, N. (1990), *"Analysis of Block Shear Experiments for Structural Steel Angles in Tension,"* Thesis presented to the University of Connecticut, in partial fulfillment of the requirements for the degree of Master of Science.

American Institute of Steel Construction (AISC)(1989), *Manual of Steel Construction, Allowable Stress Design*, 9th Edition, Chicago, IL.

American Institute of Steel Construction (AISC)(1994), *Manual of Steel Construction, Load and Resistance Factor Design*, 2nd Edition, Chicago, IL

American Institute of Steel Construction (AISC)(1999), *Load and Resistance Factor Design Specification for Structural Steel Buildings*, Chicago, IL.

Barrett, C. (2002), *"Efficiency of Tension Connections,"* Thesis presented to the University of Connecticut, at Storrs, Connecticut, in partial fulfillment of the requirements for the degree of Master of Science.

Birkemoe. P. and Gilmor, M. (1978), "Behavior of Bearing Critical Double-angle Beam Connections," *Engineering Journal*, AISC, Vol. 15, No. 4, 4th Quarter, pp. 109-115.

D'Aiuto, C. (1999), *"The Effect of Connection Geometry on the Capacity of Structural Tension Members,"* Thesis presented to the University of Connecticut, at Storrs, Connecticut, in partial fulfillment of the requirements for the degree of Master of Science.

Epstein, H. (1992), "An Experimental Study of Block Shear Failure of Angles in Tension," *Engineering Journal*, AISC, Vol. 29, No. 2, 2nd Quarter, pp. 75-84.

Epstein, H. (1996), "Block Shear of Structural Tees in Tension - Alternate Paths," *Engineering Journal*, AISC, Vol. 33, No. 4, 4th Quarter, pp. 147-152.

Epstein, H. and D'Aiuto, C. (2002), "Using Moment and Axial Interaction Equations to Account for Moment and Shear Lag Effects in Tension Members," *Engineering Journal*, AISC, Vol. 39, No. 2, 2nd Quarter, pp. 91-99.

Epstein, H. and McGinnis, M. (2000), "Finite Element Modeling of Block Shear in Structural Tees," *Computers and Structures*, Vol. 77, No. 5, pp. 571-582.

Epstein, H. and Thacker, B. (1991), "The Effect of Bolt Stagger for Block Shear Tension Failures in Angles," *Computers and Structures*, Vol. 39, No. 5, pp. 571-576.

Galambos, T.V. (1981), "Load and Resistance Factor Design," *Engineering Journal*, AISC, Vol. 18, No. 3, 3rd Quarter, pp. 74-82.

McGinnis, M. (1998), *"Analytic Studies of Block Shear Failures in Structural Tees Used in Tension,"* Thesis presented to the University of Connecticut, at Storrs, Connecticut, in partial fulfillment of the requirements for the degree of Master of Science.

Stamberg, H. (2000), *"An Improved Approach for the Code Capacity of Structural Tees in Tension,"* Thesis presented to the University of Connecticut, at Storrs, Connecticut, in partial fulfillment of the requirements for the degree of Master of Science.

Thacker, B. (1987), *"An Analytical Investigation of Block Shear Failure in Structural Steel Tension Members,"* Thesis presented to the University of Connecticut, at Storrs, Connecticut, in partial fulfillment of the requirements for the degree of Master of Science.

Twilley, R. (1996), *"An Experimental Analysis of Block Shear Failure of Structural Tees in Tension,"* Thesis submitted in partial fulfillment of the requirements for the designation of Honors Scholar at the University of Connecticut.